

RESEARCH PAPER

Using chromosome introgression lines to map quantitative trait loci for photosynthesis parameters in rice (*Oryza sativa* L.) leaves under drought and well-watered field conditions

Junfei Gu¹, Xinyou Yin¹, Paul C. Struik¹, Tjeerd Jan Stomph¹ and Huaqi Wang^{2*}

¹ Centre for Crop Systems Analysis, Department of Plant Sciences, Wageningen University, PO Box 430, 6700 AK Wageningen, The Netherlands

² Plant Breeding & Genetics, China Agricultural University, 100193 Beijing, PR China

* To whom correspondence should be addressed. Email: wanghuaqi@cau.edu.cn

Received 6 April 2011; Revised 25 July 2011; Accepted 18 August 2011

Abstract

Photosynthesis is fundamental to biomass production, but sensitive to drought. To understand the genetics of leaf photosynthesis, especially under drought, upland rice cv. Haogelao, lowland rice cv. Shennong265, and 94 of their introgression lines (ILs) were studied at flowering and grain filling under drought and well-watered field conditions. Gas exchange and chlorophyll fluorescence measurements were conducted to evaluate eight photosynthetic traits. Since these traits are very sensitive to fluctuations in microclimate during measurements under field conditions, observations were adjusted for microclimatic differences through both a statistical covariant model and a physiological approach. Both approaches identified leaf-to-air vapour pressure difference as the variable influencing the traits most. Using the simple sequence repeat (SSR) linkage map for the IL population, 1–3 quantitative trait loci (QTLs) were detected per trait–stage–treatment combination, which explained between 7.0% and 30.4% of the phenotypic variance of each trait. The clustered QTLs near marker RM410 (the interval from 57.3 cM to 68.4 cM on chromosome 9) were consistent over both development stages and both drought and well-watered conditions. This QTL consistency was verified by a greenhouse experiment under a controlled environment. The alleles from the upland rice at this interval had positive effects on net photosynthetic rate, stomatal conductance, transpiration rate, quantum yield of photosystem II (PSII), and the maximum efficiency of light-adapted open PSII. However, the allele of another main QTL from upland rice was associated with increased drought sensitivity of photosynthesis. These results could potentially be used in breeding programmes through marker-assisted selection to improve drought tolerance and photosynthesis simultaneously.

Key words: Chlorophyll fluorescence, drought, gas exchange, photosynthesis, physiological model, quantitative trait locus (QTL).

Introduction

Drought is considered to be the greatest threat to rice (*Oryza sativa* L.) production (Sharma and De Datta, 1994). The complex quantitative genetics nature of drought tolerance was once thought to be the main constraint for breeding for improved rice varieties under drought-prone environments (Nguyen *et al.*, 1997). Yet, recent evidence

has shown that progress can be made by direct selection for grain yield under managed stress trials (Bernier *et al.*, 2007; Venuprasad *et al.*, 2007, 2008; Kumar *et al.*, 2008). For further progress, indirect methods based on effective selection criteria and on molecular markers for component traits should be explored (Miura *et al.*, 2011).

Abbreviations: A, net photosynthesis rate; C_i, intercellular CO₂ concentration; DS, drought sensitivity; F, flowering stage; FS, flowering stage–drought-stressed environment; FW, flowering stage–well-watered environment; F_v/F_m, maximum efficiency of open photosystem (PS) II in the light; G, grain filling stage; GS, grain filling stage–drought-stressed environment; g_s, stomatal conductance for CO₂; GW, grain filling stage–well-watered environment; PPFD, photosynthetic photon flux density; qP, proportion of open PSII; TE, transpiration efficiency; T_{leaf}, leaf temperature; T_r, transpiration rate; Φ_{PSII}, quantum efficiency of PSII electron transport.

© 2011 The Author(s).

This is an Open Access article distributed under the terms of the Creative Commons Attribution Non-Commercial License (<http://creativecommons.org/licenses/by-nc/3.0/>), which permits unrestricted non-commercial use, distribution, and reproduction in any medium, provided the original work is properly cited.

Today unprecedented efforts are being made in dissecting complex traits into their single genetic determinants—quantitative trait loci (QTLs)—in order to support marker-assisted selection (MAS) and, eventually, cloning of genes. An increasing number of QTLs related to drought response have been reported, and these include QTLs for root morphology and other root traits such as root penetration ability (Price *et al.*, 2000, 2002; Babu *et al.*, 2003; Uga *et al.*, 2011); osmotic adjustment (Robin *et al.*, 2003); grain yield and yield components (Lanceras *et al.*, 2004; Lafitte *et al.*, 2004; Xu *et al.*, 2005); stay green (Jiang *et al.*, 2004); canopy temperature, leaf rolling and leaf drying (Yue *et al.*, 2005); and carbon isotope discrimination ($\Delta^{13}\text{C}$) (Takai *et al.*, 2009; Xu *et al.*, 2009).

Photosynthesis, being the basis of crop growth, biomass production, and yield, is one of the primary physiological processes strongly affected by drought (Chaves, 1991; Lawlor, 1995). The photosynthesis response to drought is very complex. Generally, during the onset of drought, CO_2 diffusional resistances increase, especially because stomatal aperture can change rapidly (Chaves *et al.*, 2002; Cochard *et al.*, 2002; Lawlor and Cornic, 2002). With the progress of drought and tissue dehydration, metabolic impairment will arise gradually, including a decrease in the content and activities of the major photosynthetic carbon reduction cycle enzyme, ribulose 1,5-bisphosphate carboxylase/oxygenase (Rubisco), as well as ribulose 1,5-bisphosphate (RuBP) (Reddy, 1996; Tezara *et al.*, 1999). Besides the CO_2 diffusion and CO_2 fixation pathways, photosystem II (PSII) electron transport is very susceptible to drought (Havaux, 1992; Lu and Zhang, 1999). Chlorophyll fluorescence, emitted mainly by PSII in the 680–740 nm spectral region, has been widely used for the estimation of the PSII electron transport rate *in vivo*. Combining gas exchange measurements for CO_2 fixation and chlorophyll fluorescence data for PSII electron transport may bring new insights into the regulation of photosynthesis in response to environment variables (von Caemmerer, 2000). The advent of portable open gas exchange systems integrated with chlorophyll fluorescence measuring devices enables researchers not only to measure simultaneously net photosynthetic rate (A), stomatal conductance for CO_2 (g_s), transpiration rate (T_r), intercellular CO_2 partial pressure (C_i), transpiration efficiency (TE), quantum yield of PSII (Φ_{PSII}), proportion of open PSII (qP), and maximum efficiency of open PSII in the light (F'_v/F'_m) in real time in the field, but also to keep records of microclimatic conditions during the observations such as leaf-to-air vapour pressure difference (VPD) and leaf temperature (T_{leaf}) (Long and Bernacchi, 2003).

Because of the primary importance of photosynthesis in determining crop growth, identifying QTLs controlling photosynthesis parameters is an important step in enhancing MAS for improved yield. This assertion is supported by growing evidence that there is genetic variation for photosynthetic rates among available germplasm and that recent yield progress in cereals from breeding was associated with increased photosynthesis (Fischer and Edmeades, 2010). In rice, using 20 distinct varieties, Jahn *et al.* (2011) showed

notable genetic variation in leaf photosynthetic rate. However, only a few QTL studies have been reported so far for photosynthetic traits (Teng *et al.*, 2004; Zhao *et al.*, 2008; Adachi *et al.*, 2011), probably partly because gas exchange measurements to phenotype these parameters under field conditions are laborious and phenotypes are greatly influenced by environments during growth and measurement, particularly when the microclimate unavoidably fluctuates under natural field conditions (Flood *et al.*, 2011). It is very hard to expose genotypes to exactly the same environmental conditions in terms of temperature, soil water content, and VPD. Therefore, environmental noise is usually large and obscures genetic differences, resulting in large QTL \times environment interactions or in irreproducible results (e.g. Simko *et al.*, 1999; Yin *et al.*, 1999a, b). Observations must therefore be corrected for differences in microclimate.

In this study, the aim is precision mapping of QTLs for photosynthetic parameters of rice assessed by both gas exchange and chlorophyll fluorescence under drought and well-watered field conditions. Two strategies were applied. First, an advanced backcross introgression line (IL) population was developed, which allows QTLs to be identified more precisely than the more commonly used populations such as recombinant inbred lines (RILs). Secondly, both statistical and physiological approaches to correct for microclimate variation during observations were explored, thus enhancing the precision of observed phenotypic trait values for mapping. The IL population was developed from a cross between a lowland rice and an upland rice variety, since upland rice relies exclusively on rainfall for water uptake and is generally thought to be more drought resistant.

Materials and methods

Plant materials

The mapping population consisted of 94 advanced backcross ILs. The parents were the lowland rice cv. Shennong265 (*Japonica*) and the upland rice cv. Haogelao (*Indica-Japonica* intermediate). The two cultivars were contrasting in terms of their agronomic performance under drought condition (La, 2004; Gu, 2007). Haogelao is drought tolerant, but low yielding; whereas Shennong265 is drought susceptible, but high yielding under irrigated conditions. After a cross between the two parents, the resultant F_1 plants were backcrossed with paternal cultivar Shennong265 three times, and these BC_3F_1 plants were consecutively self-pollinated five times to construct the mapping population BC_3F_6 by the single seed descent method.

DNA extraction and simple sequence repeat (SSR) analysis

Fresh leaves were collected from the BC_3F_6 lines and ground in liquid nitrogen. DNA was extracted from the ground tissue using the cetyltrimethylammonium bromide (CTAB) method (Rogers and Bendich, 1985). SSR primers were synthesized according to the sequences published by McCouch *et al.* (2002). A total volume of 25 μl of reaction mixture was composed of 1 ng μl^{-1} template DNA, 10 mmol TRIS-HCl (pH 9.0), 50 mmol KCl, 1.5 mmol MgCl_2 , 0.1% Triton X-100, 2 μmol of each primer, 2.5 mM of each dNTP (dATP, dCTP, dGTP, and dTTP), and 1 U of *Taq* DNA polymerase. Amplification was performed on a program for the initial denaturation step with 94 $^\circ\text{C}$ for 5 min, followed by 35 cycles for 1 min at 94 $^\circ\text{C}$, 1 min at 55 $^\circ\text{C}$, 2 min at 72 $^\circ\text{C}$, with a final 10 min extension at 72 $^\circ\text{C}$. The PCR products were separated on 8%

polyacrylamide denaturing gels and the bands were revealed using the silver staining protocol described by Panaud *et al.* (1996).

Phenotypic evaluation

Plants of the introgression population and recipient and donor parents were grown at the experimental station of China Agricultural University, Beijing (39°N, 116°E), China, in 2009, following a complete randomized block design, with two replications, four rows per plot (plot size 2.5 m × 1.2 m), 7.5 cm between plants within each row, and 30 cm between rows in both rainfed upland and fully irrigated lowland field conditions. The crops were managed according to standard local practice, with the following fertilizer applications: 48 kg N ha⁻¹, 120 kg P₂O₅ ha⁻¹, and 100 kg K₂O ha⁻¹ as the basal fertilizer, and additional 86 kg N ha⁻¹ at the tillering stage and 28 kg N ha⁻¹ at the booting stage. Weeds in both lowland and upland fields were controlled by a combination of chemical and manual methods, and insects were controlled chemically.

The flowering of the population occurred between 105 d and 120 d after sowing for the drought-stressed environment, and between 107 d and 119 d after sowing for the well-watered environment. Gas exchange and chlorophyll fluorescence measurements covered both flowering stage and mid-grain filling stage (~2 weeks after flowering). The measurements were adjusted by considering the flowering time and the variation of flowering time in each line to make sure each genotype had three replicates per block. For the drought-stressed environment, soil moisture was monitored with the time domain reflectometry method (TDR-TRIM-FM) at a soil depth of 0–30 cm. During the photosynthesis measurements, the soil water content was ~13–16% (v/v) at the flowering stage, and ~15–19% (v/v) at the grain-filling stage. Normally measurements were made during a clear day, between 9:00 and 11:30 h and between 13:00 and 15:00 h, with photosynthetic photon flux density (PPFD) of natural sunlight between 700 μmol m⁻² s⁻¹ and 1600 μmol m⁻² s⁻¹; *T*_{leaf} varied from 23.3 °C to 36.0 °C (Fig. 1) and relative humidity from 17.4% to 67.8% (partly shown by VPD in Fig. 1) during the measurements.

The middle parts of three fully expanded flag leaves on the main culms of three central plants in each plot were measured using a portable open gas exchange system (Li-6400, Li-COR Inc., Lincoln, NE, USA) with an integrated fluorescence chamber head (LI-6400-40, Li-COR Inc.) with a setting of PPFD at 1000 μmol m⁻² s⁻¹ and a CO₂ concentration (*C*_a) at 400 μmol CO₂ (mol air)⁻¹ by using CO₂ cylinders. Gas exchange data for net photosynthesis rate (*A*), intercellular CO₂ partial pressure (*C*_i), stomatal conductance for CO₂ (*g*_s), and transpiration rate (*T*_r), and fluorescence data for *F*_s (the steady-state fluorescence) were recorded after maintaining the leaf in the leaf chamber long enough for *A* to reach a steady state. Besides this, microclimatic data (*T*_{leaf}, VPD, etc.) were automatically recorded at the same time. Then a saturating light pulse (>8500 μmol m⁻² s⁻¹ for 0.8 s) was applied to determine *F*_m (the maximum fluorescence during the saturating light pulse). By the end, after turning off the actinic light, a 'dark pulse' (using far-red light to excite PSI preferentially and force electrons to drain from PSII) was applied to obtain *F*'₀ (the minimum fluorescence yield in the light-adapted state). From these data, three chlorophyll fluorescence parameters were derived:

- 1 $\Phi_{\text{PSII}} = (F'_m - F_s) / F'_m$, the apparent PSII e⁻ transport efficiency (Genty *et al.*, 1989), which estimates the yield of PSII photochemistry;
- 2 $qP = (F'_m - F_s) / (F'_m - F'_0)$, which quantifies the photochemical capacity of PSII (Bradbury and Baker, 1984; Quick and Horton, 1984); and
- 3 $F'_0 / F'_m = (F'_m - F'_0) / F'_m$, which quantifies the extent to which photochemistry at PSII is limited by competition with thermal decay processes (Oxborough and Baker, 1997).

From gas exchange data, TE was calculated as *A/T*_r. To assess any genetic difference in the responsiveness to drought, the ratio of

A under the drought treatment (*A*_{drought}) to that under the well-watered treatment (*A*_{water}) was calculated to indicate drought sensitivity (DS), for both flowering and grain-filling stages.

Adjusting for the effects of environmental fluctuations on trait values

As photosynthetic rate *A* or related traits (e.g. stomatal conductance) can vary greatly with environmental variables such as VPD (Cowan, 1977; Buckley and Mott, 2002), the phenotypic trait value of the *i*th genetic line was expressed in a statistical covariant model using the environmental variable as a quantitative co-regressor:

$$\mu_{ijk} = \mu + G_i + E_j + (GE)_{ij} + B_k + bx_{ijk} + e_{ijk} \quad (1)$$

where, μ =general mean; G_i =genetic effect of the *i*th genotype; E_j =treatment effect, which stands for either of the two treatments (well watered or drought stressed); $(GE)_{ij}$ =genotype × treatment interaction; B_k =the block effect; b =the effect of the environmental variable; x_{ijk} =values of the environmental variable during measurement; and e_{ijk} =residual effect. This approach allows the observed trait values to be adjusted statistically to the same value (e.g. average) of the climatic variable (*T*_{leaf} and VPD) that had inevitably fluctuated during the field measurement conditions. The analysis identified that VPD was the most influential environmental factor (see the Results).

Such a statistical approach often results in increased precision for parameter estimates and increased power for statistical tests of hypotheses (Ott and Longnecker, 2001). An alternative is to use a physiological approach (Yin *et al.*, 1999a), which helps to confirm the reliability of the statistical approach. Therefore, the use of a physiological approach, based on the photosynthesis model of Farquhar *et al.* (1980), to correct for the effects of environmental fluctuations during measurements was explored. Since *A* is Rubisco limited under the measuring conditions used (i.e. light intensity of 1000 μmol m⁻² s⁻¹ in ambient CO₂ concentration), *A* can be expressed as a consequence of CO₂ and O₂ competing for the Rubisco-binding site by carboxylation and oxygenation, respectively:

$$A = \frac{(C_i - \Gamma_*)V_{\text{cmax}}}{C_i + K_M} - R_d \quad (2)$$

where V_{cmax} is the maximum rate of Rubisco carboxylation, C_i is the intercellular CO₂ partial pressure, Γ_* is the CO₂ compensation point in the absence of day respiration (R_d), and K_M is the effective Michaelis–Menten constant. K_M is expressed as $K_{mc}(1 + O/K_{mo})$, where K_{mc} and K_{mo} are the Michaelis–Menten constants for CO₂ and O₂, respectively, and O is the oxygen concentration.

In order to incorporate the effect of VPD, the model of Ball *et al.* (1987), as modified by Leuning (1990, 1995), states that

$$g_s = g_0 + Af_{\text{vpd}} \quad (3)$$

where g_s is the stomatal conductance for CO₂ diffusion, g_0 is the residual stomatal conductance if the irradiance approaches zero, and f_{vpd} is the term for the effect of leaf-to-air VPD. f_{vpd} is expressed as $a_1 / [(C_s - \Gamma) (1 + D_s/D_o)]$, where D_s is the VPD, C_s is the CO₂ concentration at the leaf surface (which was obtained from C_a and a default value for boundary layer conductance set in the Li-Cor), a_1 and D_o are empirical coefficients, and Γ is the CO₂ compensation point, which can be derived from Equation 2 (for example, see Azcón-Bieto *et al.*, 1981) as:

$$\Gamma = \frac{\Gamma_* + K_{mc}(1 + O/K_{mo})R_d/V_{\text{cmax}}}{1 - R_d/V_{\text{cmax}}} \quad (4)$$

Combining Equations 2 and 3, and replacing C_i by $(C_s - A/g_s)$, and then solving for *A* gives

$$A = \frac{-b + \sqrt{b^2 - 4ac}}{2a} \quad (5)$$

where

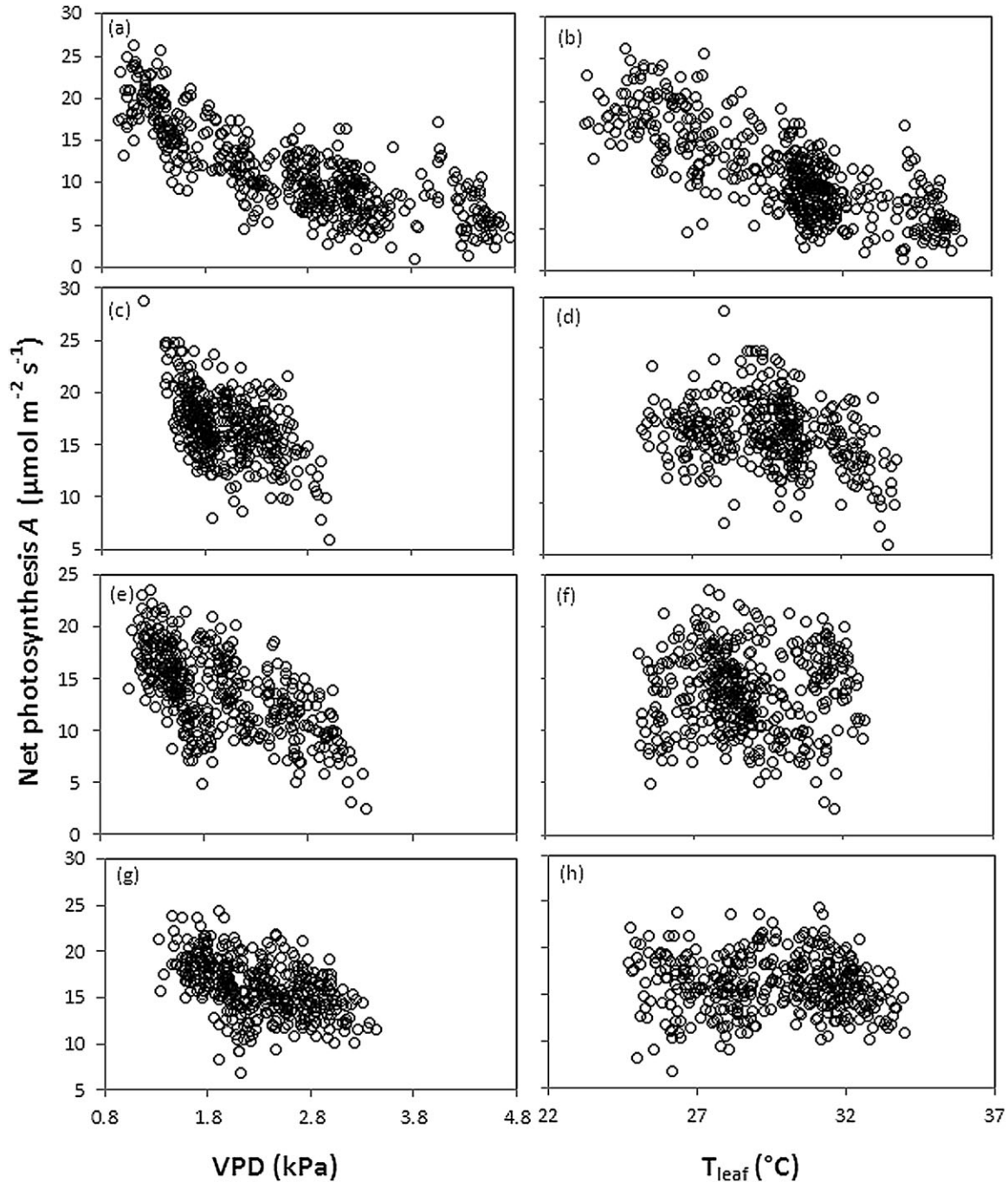


Fig. 1. Correlation between net photosynthesis A ($\mu\text{mol m}^{-2} \text{s}^{-1}$) and vapour pressure deficit VPD (the left column of plots) or T_{leaf} (the right column of plots) under different stage \times treatment combinations. At the flowering stage for drought-stressed plants (a, b) and for well-watered plants (c, d) and at mid-grain filling for drought-stressed plants (e, f) and for well-watered plants (g, h). The minimum, mean \pm SD, and maximum values are: for FS, VPD (0.96, 2.66 ± 1.01 , 4.75), T_{leaf} (23.3, 30.1 ± 3.0 , 36.0); for FW, VPD (1.21, 2.00 ± 0.35 , 3.00), T_{leaf} (25.3, 29.5 ± 1.9 , 33.9); for GS, VPD (1.07, 1.94 ± 0.56 , 3.35), T_{leaf} (25.1, 28.7 ± 1.8 , 32.7); for GW, VPD (1.32, 2.29 ± 0.47 , 3.44), T_{leaf} (24.7, 29.5 ± 2.37 , 34.0).

$$a = f_{vpd}(C_s + K_M) - 1$$

$$b = (C_s f_{vpd} + K_M f_{vpd} - 1)R_d + (C_s + K_M)g_0 - (C_s f_{vpd} - \Gamma^* f_{vpd} - 1)V_{c\max}$$

$$c = [(C_s + K_M)R_d - (C_s - \Gamma^*)V_{c\max}]g_0$$

The temperature response of the model parameters $V_{c\max}$, Γ^* , K_{mcs} , K_{mos} , and R_d are described, using a general Arrhenius equation:

$$\text{parameter} = \exp[c - \Delta H_a / (RT_K)] \quad (6)$$

where R is the molar gas constant, T_K is the leaf temperature in Kelvin, and c and ΔH_a are scaling constant and activation energy, respectively.

As constants associated with the kinetic properties of Rubisco (i.e. K_{mcs} , K_{mos} , Γ^*) are generally conservative for most higher terrestrial C_3

plants (von Caemmerer, 2000; Bernacchi *et al.*, 2001), most parameter values used in the physiological model, Equations 4–6, were derived from the literature. However, V_{cmax} and a_1 were estimated from curve fitting to the measurements for each stage×treatment combination, namely flowering–drought-stressed environment (FS), flowering–well-watered environment (FW), grain filling–drought-stressed environment (GS), and grain filling–well-watered environment (GW). All these parameters are given in Supplementary Table S1 available at *JXB* online. Using this model, measured values for A were normalized to the mean value of observed VPD and T_{leaf} for each stage×treatment combination (Supplementary Fig. S1).

Construction of a marker linkage map

The initial skeleton linkage map was constructed using MAP-MAKER/EXP3.0 (Lincoln *et al.*, 1993), based on a RIL population derived from the same parents (La, 2004). New polymorphic SSRs were also identified for the IL population. To assign all markers (including those initially identified in the RIL population) into linkage groups, the ultra-dense SSR linkage map of Temnykh *et al.* (2000) and McCouch *et al.* (2002), which contains SSRs identified in the present population, were also taken into account. Their map was used as the reference to estimate marker distances, the length of chromosomes, and the length of introgressed segments for the IL population, based on the co-linearity of markers across populations (e.g. Shen *et al.*, 2004; Wu and Huang, 2007).

QTL mapping

The significances in the difference for each trait among the ILs were tested ($P < 0.05$), and both simple and partial correlations among all the traits were estimated using SAS 9.13 to assist the analysis of any co-locations of the QTLs for various traits.

Chromosomal locations of putative QTLs for each trait were determined first by single-point analysis using the general linear model (GLM) procedure in SAS. One-way analysis of variance (ANOVA) was used to test the significance ($P < 0.01$) of association at each locus between two genotype groups (homozygous allele from Shennong265 versus that from Haogelao). Multivariate analysis of variance (MANOVA) with the PROC GLM in SAS was performed to calculate the total phenotypic variance explained by the identified QTLs of the same trait by using genotype data of the corresponding markers.

To improve the reliability of QTL analysis, MapQTL 6 software (van Ooijen, 2009) was also used to perform so-called composite interval mapping (or MQM in MapQTL 6) (Jansen, 1995). The procedure described by Yin *et al.* (2005) was followed. The threshold of QTL detection for each trait was based on 1000 permutation tests at the 5% level of significance in MapQTL 6. Regions with LOD score values between 2.0 and the calculated threshold were considered as suggestive QTLs (Lander and Kruglyak, 1995), once a suggestive region was approved by single point analysis.

Confirmation of an important QTL

From the field experiment, a QTL around marker RM410 on chromosome 9 was identified, which showed a consistent effect across treatments and stages for a number of the traits (see the Results). Therefore, during the summer of 2010, at the research facility UNIFARM, Wageningen, plants of IL161 which only contains a small segment around marker RM410 from the donor parent Haogelao, as well as the recurrent parent Shennong265, were grown in the greenhouse under controlled-environment conditions, to validate the QTL expression under an independent condition. In the greenhouse, the temperature was set at 26 °C for the 12 h light period and at 23 °C for the 12 h dark period. The CO₂ level was ~370 μmol mol⁻¹, the relative humidity was set at 65%, and extra SON-T light (providing extra PPFD of ~300 μmol m⁻² s⁻¹) was switched on when the solar radiation intensity

outside the greenhouse was <400 μmol m⁻² s⁻¹. Sixteen plants of both genotypes were grown in hydroponic culture by using half Hoagland's solution. One week before flowering, water stress was introduced by adding 12.5% polyethylene glycol (PEG-8000) (stressed condition) or not (non-stressed condition). At the flowering stage and grain-filling stage, gas exchange and chlorophyll fluorescence parameters were measured on four plants (two measurements per plant) of each treatment using the Li-Cor 6400. All measurements were made at a photon flux density of 1000 μmol m⁻² s⁻¹, ambient CO₂ concentration, VPD of 1.0–1.6 kPa, and a T_{leaf} of 25 °C.

Results

Using statistical and physiological models to correct trait values

The environmental variables, VPD and T_{leaf} , fluctuated during measurements of the large set of genotypes, especially for FS (Fig. 1); VPD ranged from 0.96 kPa to 4.75 kPa and T_{leaf} ranged from 23.3 °C to 36.0 °C. Therefore, a statistical covariant model, Equation 1, was used to adjust trait values to the mean VPD and T_{leaf} values for each stage×treatment combination. The model analysis showed that VPD had a stronger influence on trait values than did T_{leaf} . The analysis also showed that all the trait values differed significantly among the ILs for each stage×treatment combination ($P < 0.01$).

Next, a physiological model, Equations 2–6, was used to validate the covariant model by adjusting all net photosynthesis values (A) to the mean VPD and T_{leaf} of each stage×treatment combination. The results showed a tight correlation between the statistically corrected A and the physiologically corrected A ($R^2=0.92$ for FS, $R^2=0.92$ for FW, $R^2=0.99$ for GS, $R^2=0.99$ for GW) (Supplementary Fig. S2 at *JXB* online). Further analysis using the physiological model showed that the physiologically corrected A using both VPD and T_{leaf} closely correlated with A adjusted using VPD alone (Supplementary Fig. S3), confirming that VPD was the more important factor, as also indicated by the statistical model. This was probably because T_{leaf} during measurements fluctuated only around the optimum value for photosynthesis (Supplementary Fig. S1b, d, f, h), so the effect of the fluctuation on the traits, if any, was only marginal.

Phenotypic evaluations

Mean values, SDs, ranges, skewness, and kurtosis of all adjusted traits are shown in Table 1. All traits showed continuous distribution in the population and almost all showed a normal distribution with low levels of skewness and kurtosis. Compared with the two parents, ILs showed a larger range of variation (Table 1), indicating an obvious transgressive segregation. Among the traits, the relative range of variation [i.e. the coefficient of variation (CV) in Table 1] in stomatal conductance for FS was the largest, while that in the intercellular CO₂ partial pressure for FW was the smallest. Between the drought environments, the

Table 1. Statistics of photosynthesis-related traits of two parents and the population of introgression lines after adjusting to the mean VPD for each stage×treatment combination

	Traits	Unit	Haogelao	Shennong265	Introgression lines				
					Mean	CV (%)	Range	Skewness	Kurtosis
FS	A	$\mu\text{mol CO}_2 \text{ m}^{-2} \text{ s}^{-1}$	11.8	11.9	11.2	13.8	7.9–14.7	−0.06	−0.49
	g_s	$\text{mol m}^{-2} \text{ s}^{-1}$	0.091	0.094	0.089	17.5	0.061–0.128	0.11	−0.85
	T_r	$\text{mmol H}_2\text{O m}^{-2} \text{ s}^{-1}$	3.20	3.60	3.28	11.9	2.45–4.40	0.11	−0.20
	C_i	$\mu\text{mol CO}_2 \text{ mol}^{-1}$	244	248	247	6.4	206–295	0.17	0.14
	TE	$\text{mmol CO}_2 (\text{mol H}_2\text{O})^{-1}$	3.72	3.51	3.50	9.7	2.65–4.49	0.08	−0.03
	Φ_{PSII}	$\text{mol e}^- (\text{mol photon})^{-1}$	0.245	0.249	0.245	9.4	0.181–0.286	−0.39	−0.10
	qP	–	0.513	0.515	0.519	10.6	0.381–0.616	−0.43	−0.44
	F'_v/F'_m	$\text{mol e}^- (\text{mol photon})^{-1}$	0.482	0.491	0.478	5.0	0.405–0.533	−0.16	0.29
	FW	A	$\mu\text{mol CO}_2 \text{ m}^{-2} \text{ s}^{-1}$	17.6	15.4	17.1	8.6	14.3–20.6	0.15
g_s		$\text{mol m}^{-2} \text{ s}^{-1}$	0.153	0.140	0.158	8.9	0.130–0.191	0.15	−0.65
T_r		$\text{mmol H}_2\text{O m}^{-2} \text{ s}^{-1}$	4.81	4.42	4.97	8.6	3.83–5.97	0.02	−0.27
C_i		$\mu\text{mol CO}_2 \text{ mol}^{-1}$	263	271	269	2.9	251–290	0.11	−0.12
TE		$\text{mmol CO}_2 (\text{mol H}_2\text{O})^{-1}$	3.65	3.46	3.50	6.9	2.95–4.06	−0.02	−0.07
Φ_{PSII}		$\text{mol e}^- (\text{mol photon})^{-1}$	0.306	0.281	0.289	5.6	0.246–0.324	−0.06	−0.19
qP		–	0.593	0.528	0.541	6.3	0.450–0.614	−0.38	0.27
F'_v/F'_m		$\text{mol e}^- (\text{mol photon})^{-1}$	0.519	0.531	0.540	3.6	0.500–0.585	0.24	−0.71
GS		A	$\mu\text{mol CO}_2 \text{ m}^{-2} \text{ s}^{-1}$	12.6	12.6	13.7	12.1	9.85–17.3	0.00
	g_s	$\text{mol m}^{-2} \text{ s}^{-1}$	0.134	0.121	0.127	15.6	0.088–0.181	0.43	−0.04
	T_r	$\text{mmol H}_2\text{O m}^{-2} \text{ s}^{-1}$	3.82	3.39	3.68	14.8	2.63–5.37	0.36	−0.05
	C_i	$\mu\text{mol CO}_2 \text{ mol}^{-1}$	284	272	268	4.1	245–293	0.03	−0.71
	TE	$\text{mmol CO}_2 (\text{mol H}_2\text{O})^{-1}$	3.23	3.75	3.82	9.5	2.86–4.53	−0.17	−0.38
	Φ_{PSII}	$\text{mol e}^- (\text{mol photon})^{-1}$	0.246	0.247	0.267	7.7	0.219–0.313	−0.23	−0.43
	qP	–	0.466	0.455	0.531	7.6	0.424–0.615	−0.52	0.20
	F'_v/F'_m	$\text{mol e}^- (\text{mol photon})^{-1}$	0.532	0.543	0.509	5.2	0.442–0.554	−0.44	−0.35
	GW	A	$\mu\text{mol CO}_2 \text{ m}^{-2} \text{ s}^{-1}$	16.0	18.4	16.2	9.7	11.5–20.4	0.32
g_s		$\text{mol m}^{-2} \text{ s}^{-1}$	0.165	0.180	0.152	10.9	0.107–0.186	0.21	−0.27
T_r		$\text{mmol H}_2\text{O m}^{-2} \text{ s}^{-1}$	6.03	6.30	5.44	11.0	3.99–6.73	0.22	−0.47
C_i		$\mu\text{mol CO}_2 \text{ mol}^{-1}$	285	272	270	3.1	252–287	−0.14	−0.78
TE		$\text{mmol CO}_2 (\text{mol H}_2\text{O})^{-1}$	2.65	2.95	3.02	8.1	2.47–3.62	0.18	−0.45
Φ_{PSII}		$\text{mol e}^- (\text{mol photon})^{-1}$	0.292	0.281	0.278	8.0	0.212–0.343	−0.21	0.81
qP		–	0.575	0.526	0.539	9.7	0.374–0.650	−0.53	0.15
F'_v/F'_m		$\text{mol e}^- (\text{mol photon})^{-1}$	0.514	0.542	0.521	5.4	0.437–0.634	0.55	2.74
F		DS	–	0.672	0.773	0.653	13.4	0.451–0.826	−0.13
	DS	–	0.792	0.685	0.852	12.7	0.633–0.990	0.95	0.75

CV, coefficient of variation. For other definitions see the Abbreviations.

ranges of variation under drought stress were relatively larger than those in the well-watered environment, especially at flowering.

Simple and partial correlations for traits associated with gas exchange, chlorophyll fluorescence parameters, and TE are given in the bottom left and top right corners of Table 2, respectively, for each stage×treatment combination. In the simple correlation analysis, net photosynthesis (A) significantly correlated with all gas exchange and chlorophyll fluorescence parameters, except TE at grain filling, presumably reflecting the fact that photosynthesis is a complex trait associated with a number of physical and chemical reactions.

The partial correlation coefficient between g_s and A changed from 0.14 in the well-watered environment to 0.57 in the drought-stressed environment at flowering, and from 0.33 in the well-watered environment to 0.58 in the drought-stressed environment during grain filling. This shows the

direct effect of drought stress, as the CO_2 availability decreased because of diffusional limitation through stomatal closure. The significant negative correlations between C_i and A in both the simple and partial correlation analyses were also supported by Fick's first law of diffusion for CO_2 transfer along the path from C_a to C_i : $C_i = C_a - A/g_s$.

There were tight correlations between the various chlorophyll fluorescence parameters (Φ_{PSII} , qP , F'_v/F'_m) in the partial correlation analysis (Table 2). These tight correlations may reflect that Φ_{PSII} is quantitatively restricted by both qP and F'_v/F'_m (i.e. $\Phi_{\text{PSII}} = qP \times F'_v/F'_m$).

Both the correlations between A and other gas exchange parameters (g_s , T_r , C_i , and TE) and the correlations between A and chlorophyll fluorescence parameters (Φ_{PSII} , qP , and F'_v/F'_m) were significant, except between A and qP in GS (Table 2). Compared with using only gas exchange system, more information can be obtained from combining both gas

Table 2. Simple and partial correlation coefficients for traits associated with gas exchange, chlorophyll fluorescence parameters, and water use efficiency

		A	g_s	T_r	C_i	TE	Φ_{PSII}	qP	F_v/F_m
FS	<i>A</i>		0.57***	0.65***	-0.29**	0.38***	0.23*	-0.19	-0.12
	g_s	0.55***		-0.01	0.14	-0.35***	-0.41***	0.41***	0.40***
	T_r	0.69***	0.79***		0.05	-0.44***	0.13	-0.13	-0.07
	C_i	-0.58***	0.22*	0.08		-0.68***	0.04	-0.06	-0.01
	TE	0.48***	-0.34***	-0.21*	-0.94***		-0.06	0.06	0.11
	Φ_{PSII}	0.65***	0.13	0.24*	-0.66***	0.59***		0.98***	0.92***
	qP	0.32**	-0.11	-0.08	-0.58***	0.53***	0.88***		-0.96***
	F_v/F_m	0.48***	0.52***	0.60***	0.05	-0.07	-0.06	-0.52***	
	FW	<i>A</i>		0.14	0.80***	-0.08	0.46***	0.18	-0.15
g_s		0.71***		0.41***	-0.21*	-0.22*	-0.12	0.08	0.06
T_r		0.74***	0.95***		0.11	-0.38***	-0.08	0.10	0.12
C_i		-0.30**	0.35***	0.39***		-0.82***	0.01	-0.02	-0.03
TE		0.23*	-0.43***	-0.47***	-0.98***		-0.07	0.07	0.06
Φ_{PSII}		0.65***	0.34***	0.42***	-0.29**	0.25*		0.99***	0.95***
qP		0.31**	0.03	0.08	-0.30**	0.29**	0.82***		-0.98***
F_v/F_m		0.44***	0.47***	0.49***	0.09	-0.13	0.05	-0.52***	
GS		<i>A</i>		0.58***	0.68***	-0.29**	0.49***	0.13	-0.10
	g_s	0.70***		0.13	0.30**	-0.22*	-0.24*	0.22*	0.19
	T_r	0.78***	0.94***		-0.01	-0.52***	0.11	-0.10	-0.08
	C_i	-0.20*	0.50***	0.40***		-0.64***	0.12	-0.09	-0.09
	TE	0.10	-0.59***	-0.50***	-0.96***		0.06	-0.04	-0.05
	Φ_{PSII}	0.43***	-0.02	0.10	-0.45***	0.46***		0.99***	0.97***
	qP	-0.06	-0.38***	-0.34***	-0.43***	0.48***	0.75***		-0.97***
	F_v/F_m	0.67***	0.56***	0.63***	0.02	-0.10	0.26*	-0.43***	
	GW	<i>A</i>		0.33**	0.60***	-0.45***	0.22*	0.25*	-0.20
g_s		0.74***		0.51***	0.01	-0.17	-0.21	0.15	0.17
T_r		0.74***	0.98***		0.28**	-0.21*	0.04	-0.03	-0.04
C_i		-0.21*	0.46***	0.48***		-0.74***	0.15	-0.12	-0.10
TE		0.09	-0.57***	-0.58***	-0.98***		0.07	-0.05	-0.04
Φ_{PSII}		0.58***	0.20*	0.25*	-0.35***	0.31**		0.99***	0.94***
qP		0.28**	-0.08	-0.03	-0.37***	0.37***	0.87***		-0.98***
F_v/F_m		0.33***	0.47***	0.44***	0.20	-0.25*	-0.12	-0.59***	

* $P < 0.05$; ** $P < 0.01$; *** $P < 0.001$. For definitions see the Abbreviations. The simple and partial correlation coefficients are listed in the bottom left and top right corners, respectively.

exchange and chlorophyll fluorescence data, especially on the genetic diversity in electron transport components related to photosynthesis.

Construction of genetic linkage map

To obtain SSR markers showing polymorphism between Haogelao and Shennong265, >1000 SSRs were surveyed and 288 polymorphic markers were found. Among them, 130 SSR markers were evenly distributed across the genome, and were therefore chosen to construct the linkage map. The total length of the linkage map was 1645.1 cM, with an average marker spacing of 12.65 cM (Fig. 2). A graphical representation of the 130 SSRs showed that these ILs covered the whole genome of the donor parent Haogelao (Gu, 2007).

Detection of QTLs

QTL analysis for various traits was conducted separately for the four stage \times treatment combinations, by using both

single point analysis and MQM. In total, 29 QTLs were detected, including those 'suggestive' QTLs: eight QTLs for FS, eight QTLs for FW, seven QTLs for GS, three QTLs for GW, and three extra QTLs for drought sensitivity. QTLs were detected for all traits except for C_i and TE. The total fraction of the phenotypic variation explained by QTLs using genotype data of the marker at each putative QTL (single point analysis) ranged from 7.0% to 37.2%. The results are summarized in Table 3 and Fig. 2. The most significant QTLs (i.e. QTLs with LOD scores higher than the permutation calculation) are marked in bold in Table 3.

Net photosynthesis rate (*A*)

QTLs controlling net photosynthesis are located on chromosomes 2, 3, 7, 8, and 9. *A* values adjusted using the physiological model identified virtually the same QTLs (Fig. 2), again validating the statistical covariant analysis. The phenotypic variance explained by individual QTLs

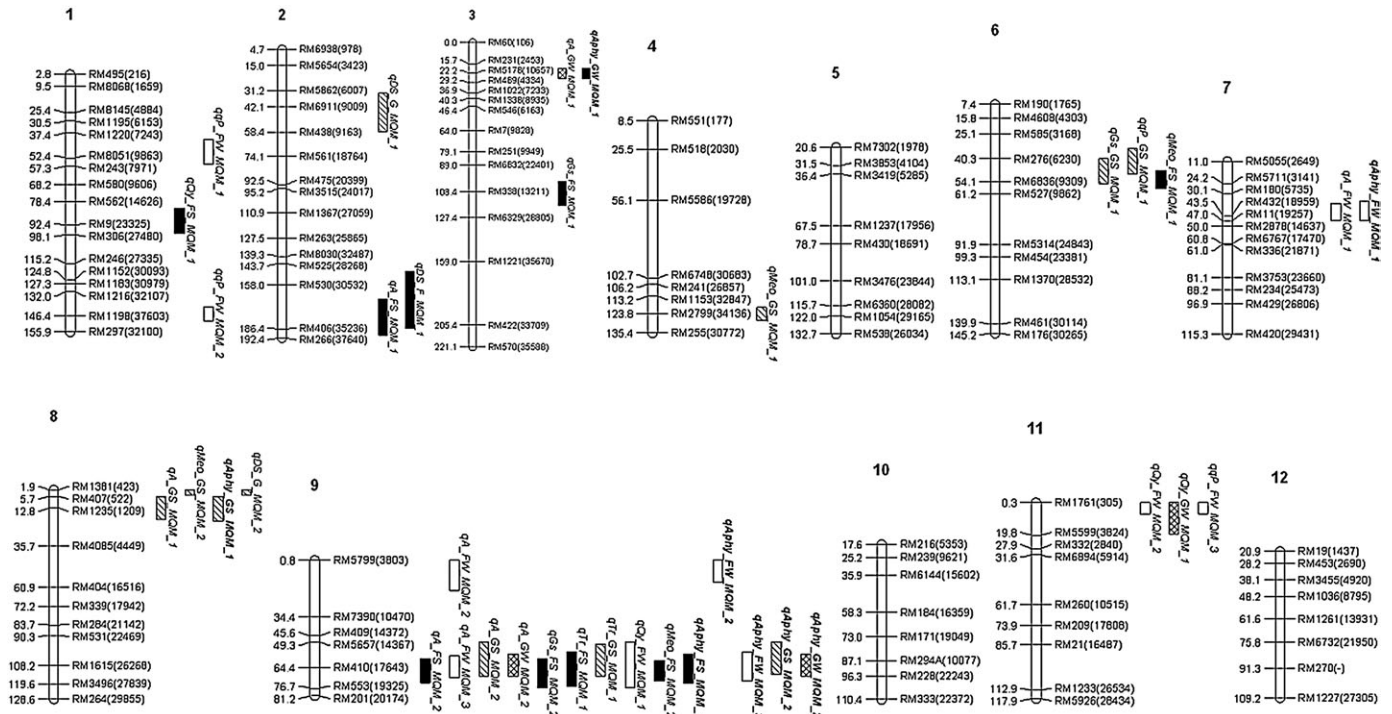


Fig. 2. Chromosome locations of QTLs associated with gas exchange and chlorophyll fluorescence data (filled bar for environment FS, open bar for FW, line-hatched bar for GS, cross-hatched bar for GW, and with the QTL name in bold for physiologically adjusted traits). The figure was drawn using software Mapchart 2.2 (Voorrips, 2002). The positions of loci are given in both cM (the number on the left) and in kb [in parentheses following the marker, based on the reference genome Nipponbare (Matsumoto *et al.*, 2005)]. The QTL position bars, placed on the right side of the chromosome, are shown in length as confidence intervals as a 1 unit decrease in LOD from the LOD profile peak. QTL nomenclature is adapted from McCouch *et al.* (1997) in the form of the q-trait-treatment-method of analysis.

varied from 7.5% to 18.2%. The additive effect ranged from $-0.92 \mu\text{mol m}^{-2} \text{s}^{-1}$ to $1.35 \mu\text{mol m}^{-2} \text{s}^{-1}$. On chromosome 9 near marker RM410, there was a QTL for all the four stage \times treatment combinations, with a consistent positive additive effect ranging from $0.55 \mu\text{mol m}^{-2} \text{s}^{-1}$ to $0.77 \mu\text{mol m}^{-2} \text{s}^{-1}$.

Stomatal conductance (g_s)

Three QTLs associated with g_s were detected on chromosomes 3 and 9 for FS, and on chromosome 6 for GS. The phenotypic variance explained by these three QTLs ranged from 9.5% to 13.5%. No QTLs were detected for well-watered conditions (FW and GW). This difference between the well-watered and stressed conditions was also shown in Table 1, which shows that the CV of g_s changed from 8.9% to 17.5% and from 10.9% to 15.6%, when comparing well-watered with stressed conditions at flowering and grain filling, respectively.

Transpiration rate (T_r)

A QTL interval was detected near marker RM410 on chromosome 9 for both FS and GS. The interval contributed to an increase of transpiration with an additive effect of $0.152 \text{ mmol m}^{-2} \text{ s}^{-1}$ and $0.244 \text{ mmol m}^{-2} \text{ s}^{-1}$, for FS and GS, respectively. The phenotypic variances explained were 10.8–11.4%. Given a tight correlation between T_r and g_s ,

the reason for no QTLs detected for g_s in well-watered conditions also applied for T_r .

Quantum yield of PSII (Φ_{PSII})

QTLs, located on chromosomes 1, 9, and 11, were found for quantum yield of PSII. The locus near marker RM1761 on chromosome 11 was consistently detected for both FW and GW. The phenotypic variance explained by these QTLs ranged from 8.6% to 10.9%, with a consistently positive effect.

Proportion of open PSII (qP)

Four QTLs associated with proportion of open PSII, located on chromosomes 1, 6, and 11, were detected. The direction of their effects was positive, except the QTL located on chromosome 1 at 146.6 cM. Individual loci explained between 8.1% and 14.2% of the phenotypic variance, and the additive effect varied from -0.011 to 0.0218 .

Maximum efficiency of open PSII in the light (F'_{v}/F'_{m})

Four QTLs related to F'_{v}/F'_{m} were detected on chromosomes 4, 6, 8, and 9 in the drought-stressed conditions, while no QTLs were found in the well-watered conditions. The total phenotypic variance explained by QTLs was 23.8% at flowering and 21.0% at grain filling. The phenotypic variance explained by individual QTLs varied from

Table 3. QTLs identified for gas exchange and chlorophyll fluorescence parameter traits in ILs from the cross Shennong 265×Haogelao under well-watered and drought-stressed environments at both flowering and grain filling stages

P -value, the significance of phenotypic variation associated with markers in single-point analysis; R^2 , the individual contribution of one QTL to the variation in a trait; global R^2 , the fraction of the total variation explained by the QTLs of the same trait; position, position of maximum LOD; LOD, logarithm of odds; a, additive allelic value of Haogelao. QTLs with LOD scores higher than the threshold set by 1000 permutation tests at 5% level of significance are marked in bold.

Traits	Stage by treatment	QTL identification	Chr	GLM/SAS				MQM			
				Marker	P -value	R^2 (%)	Global R^2	Position (cM)	LOD	R^2 (%)	a
A	FS	<i>qA_FS_MQM_1</i>	2	RM406	0.0016	11.9	30.4	180	2.26	8.1	-0.9204
		<i>qA_FS_MQM_2</i>	9	RM410	<0.0001	22.4		67.4	4.79	18.2	0.7725
	FW	<i>qA_FW_MQM_1</i>	7	RM432	0.0096	6.9	28.5	44.5	2.45	8.3	0.8307
		<i>qA_FW_MQM_2</i>	9	RM5799	0.0098	3.7		0.8	2.22	7.5	-0.6558
		<i>qA_FW_MQM_3</i>	9	RM410	0.0026	9.4		63.3	4.23	15.1	0.6408
	GS	<i>qA_GS_MQM_1</i>	8	RM1235	0.0029	9.6	15.6	10.7	2.46	10.5	-0.8627
		<i>qA_GS_MQM_2</i>	9	RM410	0.0055	8.0		57.3	2.27	9.4	0.7092
	GW	<i>qA_GW_MQM_1</i>	3	RM5178	0.0111	6.3	16.7	23.15	3.60	14.2	1.3485
		<i>qA_GW_MQM_2</i>	9	RM410	0.0008	11.5		64.3	2.85	12.2	0.5584
	g_s	<i>qGs_FS_MQM_1</i>	3	RM338	0.0086	5.9	17.6	111.4	2.30	9.5	0.0144
		<i>qGs_FS_MQM_2</i>	9	RM410	0.0009	11.1		68.4	3.30	13.8	0.0069
	GS	<i>qGs_GS_MQM_1</i>	6	RM276	0.0055	8.4	8.4	47	2.28	10.5	-0.0102
T_r	FS	<i>qTr_FS_MQM_1</i>	9	RM410	0.0006	11.9	11.9	67.4	2.47	11.4	0.1515
	GS	<i>qTr_GS_MQM_1</i>	9	RM410	0.0040	8.6	8.6	58.3	2.34	10.8	0.2436
Φ_{PSII}	FS	<i>qQy_FS_MQM_1</i>	1	RM9	0.0095	7.0	7.0	94.4	2.22	10.3	0.0111
	FW	<i>qQy_FW_MQM_1</i>	9	RM410	0.0067	7.7	10.8	58.3	2.09	8.8	0.0066
		<i>qQy_FW_MQM_2</i>	11	RM1761	0.0098	7.2		0.3	2.03	8.6	0.0085
	GW	<i>qQy_GW_MQM_1</i>	11	RM1761	0.0084	7.5	7.5	7.3	2.35	10.9	0.0155
qP	FW	<i>qqP_FW_MQM_1</i>	1	RM8051	0.0097	6.3	37.2	54.4	2.26	8.1	0.0218
		<i>qqP_FW_MQM_2</i>	1	RM1198	0.0027	9.3		146.4	2.43	9.0	-0.0111
		<i>qqP_FW_MQM_3</i>	11	RM1761	0.0047	8.5		0.3	3.71	14.2	0.0229
	GS	<i>qqP_GS_MQM_1</i>	6	RM276	0.0003	13.8	13.8	41.3	2.29	10.6	0.0181
$F'_{\sqrt{F'_m}}$	FS	<i>qMeo_FS_MQM_1</i>	6	RM6836	0.0003	13.5	23.8	55.1	3.14	12.9	-0.0122
		<i>qMeo_FS_MQM_2</i>	9	RM410	0.0016	10.2		64.4	2.33	9.3	0.0074
	GS	<i>qMeo_GS_MQM_1</i>	4	RM2799	0.0021	11.8	21.0	123.8	3.58	15.1	-0.0119
		<i>qMeo_GS_MQM_2</i>	8	RM1381	0.0097	6.2		2.9	2.05	8.3	-0.0120
DS	F	<i>qDS_F_MQM_1</i>	2	RM406	0.0010	7.0	7.0	174	2.62	11.5	-0.0640
	G	<i>qDS_G_MQM_1</i>	2	RM6911	0.0003	13.1	28.1	39.2	5.44	20.3	-0.0810
		<i>qDS_G_MQM_2</i>	8	RM1381	0.0015	10.3		1.9	3.06	10.9	-0.0525
	G	<i>qDS_G_MQM_1*2^e</i>	2*8	RM6911_1381	0.0089	5.9					

^e, epistatic interaction between two markers. For definitions see the Abbreviations.

8.3% to 15.1% with a negative effect, except for the QTL located on chromosome 9 near marker RM410.

Drought sensitivity (DS)

As indicated, DS was calculated as $A_{\text{drought}}/A_{\text{water}}$, which can characterize the relative responsiveness of each genotype to a decline in water availability. In total, three QTLs were found, one at flowering and two at grain filling. The QTLs *qDS_F_MQM_1* and *qDS_G_MQM_2* coincided with QTLs of A: *qA_FS_MQM_1* at FS and *qA_GS_MQM_1* at GS, respectively. The coincidences were expected because these loci were expressed only under one of the treatments. However, a new QTL with a relatively large effect for grain-filling stage (not detected for A at either treatments at this stage) was found on chromosome 2 with an additive effect of -0.081 on DS.

Verification of a QTL on chromosome 9 in a controlled greenhouse environment

The above QTL analysis showed that the QTL near RM410 on chromosome 9 had a significant multiple effect on A, g_s , T_r , Φ_{PSII} , and $F'_{\sqrt{F'_m}}$ across development stages and treatments. In order to assess whether the effect shown by chromosome 9 is independent and whether there is any epistasis between identified QTLs, ANOVA by PROC GLM was used to evaluate epistatic interactions between pairs of QTLs, as represented by the nearest marker loci (Lin *et al.*, 2000). There was no significant epistatic interaction found, except for DS at the grain-filling stage (Table 3). In the IL population, IL161, which had the background of recurrent parent Shennong265 except for a small introgression segment containing marker RM410 (Fig. 3a), was found; so, IL161 could serve as a near-isogenic line (NIL) of Shennong265. To

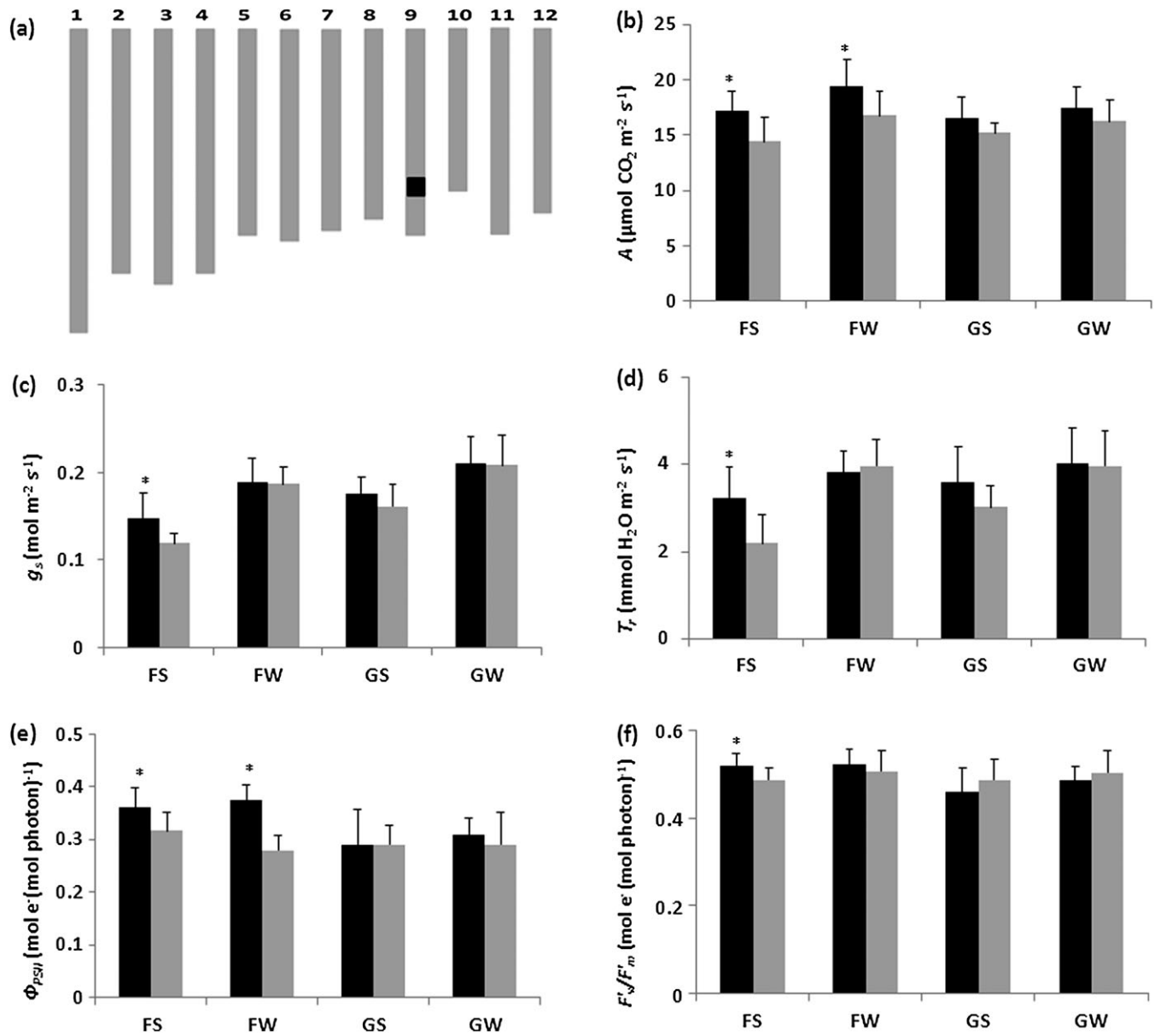


Fig. 3. Confirmation of a QTL on chromosome 9. (a) Graphical representation of genotypes of IL161. Grey bars, chromosome regions homozygous for Shennong265; black bars, chromosome region introgressed from Haogelao. The graphical genotypes shown here are based on the physical map by Matsumoto *et al.* (2005). (b–f) Comparisons of photosynthetic traits between Shennong265 (grey column) and IL161 (black column) in 2010: (b) net photosynthesis A ; (c) stomatal conductance for CO_2 g_s ; (d) transpiration rate T_r ; (e) quantum yield of PSII Φ_{PSII} ; (f) maximum efficiency of open PSII in the light F'_v/F'_m . * indicates significant differences at $P < 0.05$ between IL161 and Shennong265.

validate further the QTL near RM410, photosynthetically associated traits for Shennong265 and IL161 were measured in a greenhouse experiment. The A of IL161 was consistently higher than that of Shennong265 (Fig. 3b), confirming the positive effect of the allele from Haogelao at the locus on A . This difference was significant ($P < 0.05$) at FS and FW, which was also supported by the high LOD scores of loci $qA_FS_MQM_2$ and $qA_FW_MQM_2$, respectively. The difference was insignificant ($P > 0.05$) at GS and GW, respectively, partly in line with the comparatively small additive effects and low LOD scores of loci $qA_GS_MQM_2$ and $qA_GW_MQM_2$. For g_s , T_r , Φ_{PSII} , and F'_v/F'_m , the corresponding QTLs $qGS_FS_MQM_2$, $qTr_FS_MQM_1$,

$qQy_FW_MQM_1$, and $qMeo_FS_MQM_2$ were validated by the significant difference between IL161 and Shennong265, except for T_r at GS (Fig. 3c–f).

Discussion

In this study, the aim was to identify QTLs for photosynthetic parameters of rice under drought and well-watered field conditions during flowering and mid-grain-filling stages. Because of the limited range of genetic variation and high sensitivity to environmental perturbations, photosynthetic traits were known so far not to be amenable to

QTL analysis. Two strategies were therefore used to enhance QTL mapping precision: using both a statistical and a physiological approach to adjust phenotypic trait values for microclimatic differences during measurements in the field, and using an advanced backcross IL population. The identified QTLs tended not only to cluster in the rice genome, but also to be expressed consistently over both development stages and both drought-stressed and well-watered conditions (Fig. 2).

Complexity of photosynthetic traits

Photosynthesis as a dynamic process continuously interacts with the environment. Because of microclimate fluctuations, it is difficult to phenotype photosynthesis in the field for a large set of genotypes (Flood *et al.*, 2011). A covariant model was used here which normalized all measurements to the mean VPD, because VPD has a dominant effect on g_s and photosynthesis (Ball *et al.*, 1987; Leuning, 1990, 1995). This dominant effect of VPD, relative to T_{leaf} , was confirmed by the statistical analysis. Bernacchi *et al.* (2001), however, demonstrated that T_{leaf} influenced many aspects of the biochemical and biophysical reactions which determine the rate of photosynthesis. Using a physiological model, the mixed effects of VPD and T_{leaf} could be separated (Supplementary Fig. S1 at *JXB* online). A sensitivity analysis with and without considering temperature effect showed that A was little affected by T_{leaf} but strongly affected by VPD (Supplementary Fig. S3). Part of the reason may be that temperature during measurements varied around the optimum temperature of photosynthesis ($\sim 30^\circ\text{C}$), where the temperature response is less prominent (Supplementary Fig. S1). Partly because $\text{VPD} = e(T_{\text{leaf}}) - e_a$, where $e(T_{\text{leaf}})$ is the saturation vapour pressure based on T_{leaf} and e_a is the vapour pressure in the ambient air. The equation indicates that T_{leaf} may influence photosynthesis through VPD. Therefore, the physiological model confirmed the covariant model analysis in separating the mixed effects of VPD and T_{leaf} based on solid physiological principles.

The QTL study using corrected trait values showed that <35% of the QTLs for chlorophyll fluorescence parameters coincided with those for gas exchange parameters (Table 3). Chlorophyll fluorescence parameters indicate the electron transport capacity of photosynthesis (Genty *et al.*, 1989). Different QTLs identified for chlorophyll fluorescence and gas exchange parameters suggest that photosynthetic electron transport and CO_2 fixation are not entirely coupled. The partial uncoupling between the two sets of parameters could be due to the fact that A was limited by the Rubisco activity during the measurement conditions ($\text{PPFD} = 1000 \mu\text{mol m}^{-2} \text{s}^{-1}$); in this state, part of the electrons were used for processes other than CO_2 fixation (Yin *et al.*, 2006, 2009). The alternative use of electrons could be especially the case when plants are facing drought stress (Chaves, 1991). During onset of water stress, stomatal aperture will first decrease to reduce the water loss; this sensitivity of stomatal conductance was also shown in the present data (Table 1), with more variance in drought conditions than in

well-watered conditions. Net photosynthesis will be reduced after the stomatal response as a consequence of the reduced C_i . A further complication under drought is the associated increase in T_{leaf} . High temperature will have feedback effects: first, by increasing transpiration as a result of an increased VPD at the leaf surface. Secondly, high T_{leaf} may alter the biochemical activity of photosynthetic enzymes (e.g. V_{cmax}). Thirdly, the higher canopy temperature may accelerate ageing of the leaf, thus shortening the growing period. The complex and conflicting responses of gas exchange and electron transport to drought stress mean that physiological knowledge should be incorporated into genetic analysis of photosynthesis.

Merits of an IL population

Since Eshed and Zamir (1994) constructed the first complete set of ILs in tomato carrying single *Lycopersicon pennellii* chromosomal segments into a homogeneous background of *Lycopersicon esculentum* (now *Solanum lycopersicum*) representing the entire wild tomato genome, ILs also became popular in other crop species such as rice, potato, and barley, and in the model plant *Arabidopsis*. ILs are plant series that possess segments of the donor parent chromosome in the background of the recurrent parent. These ILs can be considered similar to a genomic library with genome inserts. The ability to identify small phenotypic effects statistically is increased by the removal of background noise. Also the homozygous lines are immortal, and phenotypic data can be obtained from different environments (e.g. across various years).

In the present IL population there was an line, IL161, with only a single desirable segment introgressed, the interval on chromosome 9, with co-location QTLs of A , g_s , T_r , Φ_{PSII} , and F^2_v/F^2_m . Because all phenotypic variance between the IL and the recurrent parent (cv. Shennong265) is due to the introgressed segment, the detection of this QTL was validated by comparing the difference in photosynthetic traits between IL161 and Shennong265 in an independent environment (Fig. 3). Because the greenhouse microenvironment variables (temperature, humidity, light intensity, etc.) were controlled at relatively constant levels, the results of the greenhouse experiment for QTL verification implicitly proved the efficacy of the covariant and physiological models in adjusting phenotypic trait values for field microclimatic differences to produce a more accurate QTL analysis.

Clusters of QTLs

The phenomenon of QTL clusters has been observed in different crops, including rice (Xiao *et al.*, 1996), barley (*Hordeum vulgare* L.) (Yin *et al.*, 1999b), wheat (*Triticum aestivum* L.) (Quarrie *et al.*, 2006), cotton (*Gossypium hirsutum* L.) (Shapley *et al.*, 1998), soybean (*Glycine max* L.) (Xu *et al.*, 2011), sorghum [*Sorghum bicolor* (L.) Moench] (Lin *et al.*, 1995), and peach (*Prunus persica* L.) (Quilot *et al.*, 2004). This clustering may be due to the tight

linkage of genes or to the pleiotropic effects of a single locus. By using substitution mapping, Monforte and Tanksley (2000) demonstrated in *S. lycopersicum* L. that a region affecting several agronomically important traits actually resulted from the linkage of multiple QTLs. However, Xue *et al.* (2008) showed that the tight correlation between the number of grains per panicle, plant height, and heading date was due to the pleiotropic effect of a single QTL *Ghd7*.

In the present study, four intervals located on chromosomes 6, 8, 9, and 11 were found to control two or more photosynthetic traits each. Especially in the interval from 57.3 cM to 68.4 cM of chromosome 9 (~2500 kb), QTLs related to A , g_s , T_r , Φ_{PSII} , and F_v/F_m were clustered and showed the same positive effect from the allele of upland rice Haogelao. Knowledge of the photosynthetic processes that chloroplast electron transport rates and carbon metabolism are coupled (at least to some extent), suggesting that pleiotropic effects are likely. A conclusion about whether the clustering is caused by pleiotropy or by gene linkage within these QTL regions cannot be reached at this stage. For better characterization of these loci, it is necessary to reduce the extent of introgression and develop NILs carrying fine-mapped QTLs.

The clustering of QTLs also indicates the difficulties of manipulating correlated traits simultaneously. For example, TE is an important target for breeding (Xu *et al.*, 2009). From a theoretical perspective, Condon *et al.* (2004) indicated that under certain environment conditions, leaf-level TE could be improved by higher photosynthetic potential, lower stomatal conductance, or a combination of these two. However, in the present experiment, the clustering of QTLs for A and g_s on chromosome 9 shows that the photosynthesis was improved by keeping stomata more open, resulting in higher C_i , and higher photosynthesis (Fig. 3). This association means a higher loss of water at the same time, thereby keeping TE virtually invariant. This could be the reason why there was no QTL found for TE near marker RM410. Again, further analysis based on finer substitution lines might answer the question of whether the association among A , g_s , and T_r could be broken towards a significantly improved TE.

Marker-assisted selection

The above interesting QTL clusters in the IL population for a number of traits could be explored for further MAS for an improved photosynthetic performance. In particular, the QTL at the RM410 locus was independently confirmed, showing a positive allele from upland rice Haogelao. The upland rice cultivar generally performed better under drought for a number of agronomic traits (La, 2004; Gu, 2007). The present result indicates the possibility of simultaneous improvement of drought tolerance and photosynthetic traits. For breeders, it is interesting to identify co-locations of QTLs, especially when their effects have the same positive direction. This co-location could potentially

be used in a breeding programme through MAS to combine multiple benefits without negative effects.

The analysis with DS (expressed as $A_{\text{drought}}:A_{\text{water}}$) identified additional QTLs (Table 3), especially *qDS_G_MQM_1* which has the highest LOD score (5.44) in the present study. For breeding one would select for genotypes which have not only high photosynthetic rates but also low photosynthetic sensitivity to drought. QTLs for DS all had negative additive effects (Table 3), indicating that alleles from Haogelao were surprisingly associated with high sensitivity to drought. Nevertheless, the ILs are good ready breeding materials which are most like the recurrent parents but are further improved by the introgression of desired traits from the donor plant. Further rounds of selection on the basis of these ILs, using the markers associated with the QTLs, could combine favourable alleles of multiple loci into a single genotype.

Concluding remarks

This is the first paper using simultaneously measured gas exchange and chlorophyll fluorescence data to study intensively the genetic differences in photosynthesis under field conditions. A physiological model to support the covariant model was also introduced to remove the microenvironment variation noise. Through these approaches, consistent results across environments and growth stages were obtained, and co-location of physiologically tightly related QTLs was observed. A QTL controlling multiple photosynthetic traits identified under field conditions was then successfully confirmed. In view of climate change (CO_2 enrichment, higher temperatures, and more severe drought stress), photosynthesis as a source of crop production is directly influenced by these factors, and has also been considered as the only remaining major trait available to increase crop yield potential further (Long *et al.*, 2006; Murchie *et al.*, 2009; Zhu *et al.*, 2010). Fischer and Edmeades (2010) have shown that recent yield progress in cereals from breeding was associated with increased photosynthesis. It is expected that photosynthesis will receive increasing attention in genetic studies and future breeding programmes (e.g. Adachi *et al.*, 2011). A great challenge for drought-prone environments is to increase the photosynthetic rate and transpiration efficiency simultaneously. To that end, rich physiological knowledge should be explored to enhance the genetic analysis of the traits of photosynthesis and water use, as already illustrated for other traits (e.g. Yin *et al.*, 1999a; Bertin *et al.*, 2010). The present results highlight that combined physiological and genetic tools can be helpful to improve screening and selection strategies in rice breeding for increased photosynthesis under field conditions

Supplementary data

Supplementary data are available at *JXB* online.

Table S1. The values of photosynthetic parameters used in the physiological adjustment.

Figure S1. Percentage deviation of net photosynthesis rate (A) to VPD and T_{leaf} predicted by the physiological model for four different stage–treatment combinations.

Figure S2. Comparison between physiologically adjusted net photosynthesis rate (A) and the statistically adjusted A .

Figure S3. Comparison between the physiologically adjusted net photosynthesis rate (A , $\mu\text{mol CO}_2 \text{ m}^{-2} \text{ s}^{-1}$) and mean VPD and the physiologically adjusted A to both mean VPD and T_{leaf} .

Acknowledgements

JG thanks the China Scholarship Council for granting him a PhD scholarship.

References

- Adachi S, Tsuru Y, Nito N, Murata K, Yamamoto T, Ebitani T, Ookawa T, Hirasawa T.** 2011. Identification and characterization of genomic regions on chromosomes 4 and 8 that control the rate of photosynthesis in rice leaves. *Journal of Experimental Botany* **62**, 1927–1938.
- Azcón-Bieto J, Farquhar GD, Caballero A.** 1981. Effects of temperature, oxygen concentration, leaf age and seasonal variations on the CO_2 compensation point of *Lolium perenne* L. *Planta* **152**, 497–504.
- Babu RC, Nguyen BD, Chamarek V, et al.** 2003. Genetic analysis of drought resistance in rice by molecular markers: association between secondary traits and field performance. *Crop Science* **43**, 1457–1469.
- Ball JT, Woodrow IE, Berry JA.** 1987. A model predicting stomatal conductance and its contribution to the control of photosynthesis under different environmental conditions. In: Biggins J, ed. *Progress in photosynthesis research*, Vol. IV. Dordrecht, The Netherlands: Martinus-Nijhoff Publishers, 221–224.
- Bernacchi CJ, Singaas EL, Pimentel C, Portis AR, Long SP.** 2001. Improved temperature response functions for models of Rubisco-limited photosynthesis. *Plant, Cell and Environment* **24**, 253–259.
- Bernier J, Kumar A, Ramaiah V, Spaner D, Atlin G.** 2007. A large-effect QTL for grain yield under reproductive-stage drought stress in upland rice. *Crop Science* **47**, 507–516.
- Bertin N, Martre P, Génard M, Quilot B, Salon C.** 2010. Under what circumstances can process-based simulation models link genotype to phenotype for complex traits? Case-study of fruit and grain quality traits. *Journal of Experimental Botany* **61**, 955–967.
- Bradbury M, Baker NR.** 1984. A quantitative determination of photochemical and non-photochemical quenching during the slow phase of the chlorophyll fluorescence induction curve of bean leaves. *Biochimica et Biophysica Acta* **765**, 275–281.
- Buckley TN, Mott KA.** 2002. Stomatal water relations and the control of hydraulic supply and demand. *Progress in Botany* **63**, 309–325.
- Chaves MM.** 1991. Effects of water deficits on carbon assimilation. *Journal of Experimental Botany* **42**, 1–16.
- Chaves MM, Pereira JS, Maroco J, Rodrigues ML, Ricardo CPP, Osório ML, Carvalho I, Faria T, Pinheiro C.** 2002. How plants cope with water stress in the field? Photosynthesis and growth. *Annals of Botany* **89**, 907–916.
- Cochard H, Lluís C, Le RX, Thierry A.** 2002. Unraveling the effects of plant hydraulics on stomatal closure during water stress in walnut. *Plant Physiology* **128**, 282–290.
- Condon AG, Richards RA, Rebetzke GJ, Farquhar GD.** 2004. Breeding for high water-use efficiency. *Journal of Experimental Botany* **55**, 2447–2460.
- Cowan IR.** 1977. Stomatal behavior and environment. *Advances in Botanical Research* **4**, 117–228.
- Eshed Y, Zamir D.** 1994. Introgressions from *Lycopersicon pennellii* can improve the soluble-solids yield of tomato hybrids. *Theoretical and Applied Genetics* **88**, 891–897.
- Farquhar GD, von Caemmerer S, Berry JA.** 1980. A biochemical model of photosynthetic CO_2 assimilation in leaves of C_3 species. *Planta* **149**, 78–90.
- Fischer RA, Edmeades GO.** 2010. Breeding and cereal yield progress. *Crop Science* **50**, 85–98.
- Flood PJ, Harbinson J, Aarts MGM.** 2011. Natural genetic variation in plant photosynthesis. *Trends in Plant Science* **16**, 327–335.
- Genty B, Briantais JM, Baker NR.** 1989. The relationship between the quantum yield of photosynthetic electron transport and quenching of chlorophyll fluorescence. *Biochimica et Biophysica Acta* **990**, 87–92.
- Gu J.** 2007. Development of introgression lines of upland rice (*Oryza sativa* L.) and QTLs mapping on root traits. Master dissertation. China Agricultural University.
- Havaux M.** 1992. Stress tolerance of photosystem II *in vivo*: antagonistic effects of water, heat, and photoinhibition stresses. *Plant Physiology* **100**, 424–432.
- Jahn CE, McKay JK, Mauleon R, Stephens J, McNally K, Bush DR, Leung H, Leach JE.** 2011. Genetic variation in biomass traits among 20 diverse rice varieties. *Plant Physiology* **155**, 157–168.
- Jansen RC.** 1995. Genetic mapping quantitative trait loci in plants: a novel statistical approach. PhD dissertation, Wageningen University, The Netherlands.
- Jiang GH, He YQ, Xu CG, Li XH, Zhang Q.** 2004. The genetic basis of stay-green in rice analysed in a population of doubled haploid lines derived from an *indica* by *japonica* cross. *Theoretical and Applied Genetics* **108**, 688–698.
- Kumar A, Bernier J, Verulkar S, Lafitte HR, Atlin GN.** 2008. Breeding for drought tolerance: direct selection for yield, response to selection and use of drought-tolerant donors in upland and lowland-adapted populations. *Field Crops Research* **107**, 221–231.
- La H.** 2004. The QTL mapping of traits related to drought tolerance and genetic transformation of herbicide tolerance in rice (*Oryza sativa* L.). Dissertation. China Agricultural University.
- Lafitte HR, Price AH, Courtois B.** 2004. Yield response to water deficit in an upland rice mapping population: associations among traits and genetic markers. *Theoretical and Applied Genetics* **109**, 1237–1246.
- Lanceras JC, Pantuwan G, Jongdee B, Toojinda T.** 2004. Quantitative trait loci associated with drought tolerance at reproductive stage in rice. *Plant Physiology* **135**, 384–399.

- Lander E, Kruglyak L.** 1995. Genetic dissection of complex traits: guidelines for interpreting and reporting linkage results. *Nature Genetics* **11**, 241–247.
- Lawlor DW.** 1995. The effects of water deficit on photosynthesis. In: Smirnoff N, ed. *Environment and plant metabolism Flexibility and acclimation*. Oxford: BIOS Scientific Publishers, 129–160.
- Lawlor DW, Cornic G.** 2002. Photosynthetic carbon assimilation and associated metabolism in relation to water deficits in higher plants. *Plant, Cell and Environment* **25**, 275–294.
- Leuning R.** 1990. Modelling stomatal behaviour and photosynthesis of *Eucalyptus grandis*. *Australian Journal of Plant Physiology* **17**, 159–175.
- Leuning R.** 1995. A critical appraisal of a combined stomatal photosynthesis model for C_3 plants. *Plant, Cell and Environment* **18**, 339–355.
- Lin HX, Yamamoto T, Sasaki T, Yano M.** 2000. Characterization and detection of epistatic interactions of 3 QTLs, Hd1, Hd2, and Hd3, controlling heading date in rice using nearly isogenic lines. *Theoretical and Applied Genetics* **101**, 1021–1028.
- Lin YR, Schertz KF, Paterson AH.** 1995. Comparative analysis of QTL affecting plant height and maturity across Poaceae, in reference to an interspecific sorghum population. *Genetics* **141**, 391–411.
- Lincoln S, Daly M, Lander E.** 1993. *MAPMAKER/EXP 3.0 and MAPMAKER/QTL 1.1. Technical report*. Cambridge, MA: Whitehead Institute of Medical Research.
- Long SP, Bernacchi CJ.** 2003. Gas exchange measurements, what can they tell us about the underlying limitations to photosynthesis? Procedures and source error. *Journal of Experimental Botany* **54**, 2393–2401.
- Long SP, Zhu XG, Naidu S, Ort DR.** 2006. Can improvement in photosynthesis increase crop yields? *Plant, Cell and Environment* **29**, 315–330.
- Lu C, Zhang J.** 1999. Effects of water stress on photosystem II photochemistry and its thermostability in wheat plants. *Journal of Experimental Botany* **50**, 1199–1206.
- Matsumoto T, Wu JZ, Kanamori H, et al.** 2005. The map-based sequence of the rice genome. *Nature* **436**, 793–800.
- McCouch SR, Cho YG, Yano M, Paul E, Blinstrub M.** 1997. Report on QTL nomenclature. *Rice Genetics Newsletter* **14**, 11–13.
- McCouch SR, Teytelman L, Xu Y, et al.** 2002. Development and mapping of 2240 new SSR markers for rice (*Oryza sativa* L.). *DNA Research* **9**, 199–207.
- Miura K, Ashikari M, Matsuoka M.** 2011. The role of QTLs in the breeding of high-yielding rice. *Trends in Plant Science* **16**, 319–326.
- Monforte AJ, Tanksley SD.** 2000. Fine mapping of a quantitative trait locus (QTL) from *Lycopersicon hirsutum* chromosome 1 affecting fruit characteristics and agronomic traits: breaking linkage among QTLs affecting different traits and dissection of heterosis for yield. *Theoretical and Applied Genetics* **100**, 471–479.
- Murchie EH, Pinto M, Horton P.** 2009. Agriculture and the new challenges for photosynthesis research. *New Phytologist* **181**, 532–552.
- Nguyen HT, Chandra BR, Blum A.** 1997. Breeding for drought resistance in rice: physiology and molecular genetics considerations. *Crop Science* **37**, 1426–1434.
- Ott RL, Longnecker M.** 2001. *An introduction to statistical methods and data analysis*, 5th edn. California: Duxbury.
- Oxborough K, Baker NR.** 1997. Resolving chlorophyll a fluorescence image of photosynthetic efficiency into photochemical and non-photochemical component calculation of qP and F'_v/F'_m without measuring F'_o . *Photosynthesis Research* **54**, 135–142.
- Panaud O, Chen X, McCouch SR.** 1996. Development of microsatellite markers and characterization of simple sequence length polymorphism (SSLP) in rice (*Oryza sativa* L.). *Molecular and General Genetics* **252**, 597–607.
- Price AH, Cairns JE, Horton P, Jones HG, Griffiths H.** 2002. Linking drought-resistance mechanisms to drought avoidance in upland rice using a QTL approach: progress and new opportunities to integrate stomatal and mesophyll responses. *Journal of Experimental Botany* **53**, 989–1004.
- Price AH, Steele KA, Moore BJ, Barraclough PB, Clark LJ.** 2000. A combined RFLP and AFLP linkage map of upland rice (*Oryza sativa* L.) used to identify QTLs for root-penetration ability. *Theoretical and Applied Genetics* **100**, 49–56.
- Quarrie SA, Quarrie SP, Radosevic R, Rancic D, Kaminska A, Barnes JD, Leverington M, Ceoloni C, Dodig D.** 2006. Dissecting a wheat QTL for yield present in a range of environments: from the QTL to candidate genes. *Journal of Experimental Botany* **57**, 2627–2637.
- Quick WP, Horton P.** 1984. Studies on the induction of chlorophyll fluorescence in barley protoplasts. II Resolution of fluorescence quenching by redox state and the transthylakoid pH gradient. *Proceedings of the Royal Society B: Biological Sciences* **220**, 371–382.
- Quilot B, Wu BH, Kervella J, Génard M, Foulongne M, Moreau K.** 2004. QTL analysis of quality traits in an advanced backcross between *Prunus persica* cultivars and the wild relative species. *P. davidiana*. *Theoretical and Applied Genetics* **109**, 884–897.
- Reddy AR.** 1996. Fructose 2,6-bisphosphate-modulated photosynthesis in sorghum leaves grown under low water regimes. *Phytochemistry* **43**, 19–22.
- Robin S, Pathan MS, Courtois B, Lafitte R, Carandang S, Lanceras S, Amante M, Nguyen HT, Li Z.** 2003. Mapping osmotic adjustment in an advanced back-cross inbred population of rice. *Theoretical and Applied Genetics* **107**, 1288–1296.
- Rogers OS, Bendich AJ.** 1985. Extraction of DNA from milligram amounts of fresh, herbarium and mummified plant tissues. *Plant Molecular Biology* **5**, 69–76.
- Shappley ZW, Jenkins JN, Zhu J, McCarty JC.** 1998. Quantitative trait loci associated with yield and fiber traits of upland cotton. *Journal of Cotton Science* **4**, 153–163.
- Sharma PK, De Datta SK.** 1994. Rain water utilization efficiency in rain-fed lowland rice. *Advances in Agronomy* **52**, 85–120.

- Shen YJ, Jiang H, Jin JP, et al.** 2004. Development of genome-wide DNA polymorphism database for map-based cloning of rice genes. *Plant Physiology* **135**, 1198–1205.
- Simko I, Vreugdenhil D, Jung CS, May GD.** 1999. Similarity of QTLs detected for *in vitro* and greenhouse development of potato plants. *Molecular Breeding* **5**, 417–428.
- Takai T, Ohsumi A, San-oh Y, Laza MRC, Kondo M, Yamamoto T, Yano M.** 2009. Detection of a quantitative trait locus controlling carbon isotope discrimination and its contribution to stomatal conductance in *japonica* rice. *Theoretical and Applied Genetics* **118**, 1401–1410.
- Temnykh S, Park WD, Ayres N, Cartinhour S, Hauck N, Lipovich L, Cho YG, Ishii T, McCouch SR.** 2000. Mapping and genome organization of microsatellite sequences in rice (*Oryza sativa* L.). *Theoretical and Applied Genetics* **100**, 697–712.
- Teng S, Qian Q, Zeng D, Kunihiro Y, Fujimoto K, Huang D, Zhu L.** 2004. QTL analysis of leaf photosynthetic rate and related physiological traits in rice (*Oryza sativa* L.). *Euphytica* **135**, 1–7.
- Tezara W, Mitchell VJ, Driscoll SD, Lawlor DW.** 1999. Water stress inhibits plant photosynthesis by decreasing coupling factor and ATP. *Nature* **401**, 914–917.
- Uga Y, Okuno K, Yano M.** 2011. *Dro1*, a major QTL involved in deep rooting of rice under upland field conditions. *Journal of Experimental Botany* **62**, 2485–2494.
- van Ooijen JW.** 2009. *MapQTL® 6. Software for the mapping of quantitative trait loci in experimental populations of diploid species*. Wageningen, The Netherlands: Kyazma BV.
- Venuprasad R, Lafitte HR, Atlin GN.** 2007. Response to direct selection for grain yield under drought stress in rice. *Crop Science* **47**, 285–293.
- Venuprasad R, Sta Cruz MT, Amante M, Magbanua R, Kumar A, Atlin GN.** 2008. Response to two cycles of divergent selection for grain yield under drought stress in four rice breeding populations. *Field Crops Research* **107**, 232–244.
- von Caemmerer S.** 2000. *Biochemical models of leaf photosynthesis*. Australia: CSIRO Publishing.
- Voorrips RE.** 2002. MapChart: software for the graphical presentation of linkage maps and QTLs. *Journal of Heredity* **93**, 77–78.
- Wu YQ, Huang Y.** 2007. An SSR genetic map of *Sorghum bicolor* (L.) Moench and its comparison to a published genetic map. *Genome* **50**, 84–89.
- Xiao J, Li J, Yuan L, Tanksley SD.** 1996. Identification of QTLs affecting traits of agronomic importance in a recombinant inbred population derived from a subspecific rice cross. *Theoretical and Applied Genetics* **92**, 230–244.
- Xu JL, Lafitte HR, Gao YM, Fu BY, Torres R, Li ZK.** 2005. QTLs for drought escape and tolerance identified in a set of random introgression lines of rice. *Theoretical and Applied Genetics* **111**, 1642–1650.
- Xu Y, Li HN, Li GJ, Wang X, Cheng LG, Zhang YM.** 2011. Mapping quantitative trait loci for seed size traits in soybean (*Glycine max* L. Merr.). *Theoretical and Applied Genetics* **122**, 581–594.
- Xu YB, This D, Pausch RC, Vonhof W, Coburn JR, Comstock JP, McCouch SR.** 2009. Leaf-level water use efficiency determined by carbon isotope discrimination in rice seedlings: genetic variation associated with population structure and QTL mapping. *Theoretical and Applied Genetics* **118**, 1065–1081.
- Xue W, Xing Y, Weng X, et al.** 2008. Natural variation in *Ghd7* is an important regulator of heading date and yield potential in rice. *Nature Genetics* **40**, 761–767.
- Yin X, Harbinson J, Struik PC.** 2006. Mathematical review of literature to assess alternative electron transports and interphotosystem excitation partitioning of steady-state C₃ photosynthesis under limiting light. *Plant, Cell and Environment* **29**, 1771–1782.
- Yin X, Harbinson J, Struik PC.** 2009. A model of the generalized stoichiometry of electron transport-limited C₃ photosynthesis. In: Laik A, Nedbal L, Govindjee, eds. *Photosynthesis in silico: understanding complexity from molecules to ecosystems. Advances in photosynthesis and respiration* vol. 29. Dordrecht The Netherlands: Springer, 247–273.
- Yin X, Kropff MJ, Stam P.** 1999a. The role of ecophysiological models in QTL analysis: the example of specific leaf area in barley. *Heredity* **82**, 415–421.
- Yin X, Stam P, Dourleijn CJ, Kropff MJ.** 1999b. AFLP mapping of quantitative trait loci for yield-determining physiological characters in spring barley. *Theoretical and Applied Genetics* **99**, 244–253.
- Yin X, Struik PC, van Eeuwijk FA, Stam P, Tang J.** 2005. QTL analysis and QTL-based prediction of flowering phenology in recombinant inbred lines of barley. *Journal of Experimental Botany* **56**, 967–976.
- Yue B, Xiong L, Xue W, Xing Y, Luo L, Xu C.** 2005. Genetic analysis for drought resistance of rice at reproductive stage in field with different types of soil. *Theoretical and Applied Genetics* **111**, 1127–1136.
- Zhao X, Xu J, Zhao M, Lafitte R, Zhu L, Fu B, Gao Y, Li Z.** 2008. QTLs affecting morphophysiological traits related to drought tolerance detected in overlapping introgression lines of rice (*Oryza sativa* L.). *Plant Science* **174**, 618–625.
- Zhu XG, Long SP, Ort DR.** 2010. Improving photosynthetic efficiency for great yield. *Annual Review of Plant Biology* **61**, 235–261.